Pergamon

Acta mater. 49 (2001) 3277–3287

Acta MATERIALIA

www.elsevier.com/locate/actamat

ON THE ORIGIN OF DEFORMATION MICROSTRUCTURES IN AUSTENITIC STAINLESS STEEL: PART II—MECHANISMS

E. H. LEE†, M. H. YOO, T. S. BYUN, J. D. HUNN, K. FARRELL‡ and L. K. MANSUR

Metals and Ceramics Division, Oak Ridge National Laboratory, PO Box 2008, Oak Ridge, TN 37831-6376, USA

(Received 23 January 2001; accepted 11 May 2001)

Abstract—Deformation microstructures of austenitic stainless steels consist of profuse pile-up dislocations, stacking faults, nanotwins, and defect-reduced channels as demonstrated in the Part I companion paper of this title [*Acta mater.*, 2001, **49**(16), 3269–3276]. Yet the mechanisms of such microstructural evolution are poorly understood. Thus, a comprehensive study was conducted to understand the underlying physics of deformation in metals using radiation damage as a tool. It was found that, for energetic reasons, glide dislocations dissociated into Shockley partials during glide. Consequently, the interaction between a glide dislocation and radiation-induced defects occurs by a two-step reaction, first with the leading partial and then with the trailing partial. With this insight, the origin of deformation microstructures was explained by analyzing Shockley partial dislocations and their interactions with radiation-induced Frank loops. © *2001 Acta Materialia Inc. Published by Elsevier Science Ltd. All rights reserved.*

Keywords: Steels (austenite); Deformation mechanisms

1. INTRODUCTION

In general, the microstructure of irradiated austenitic stainless steels is characterized by profuse Frank interstitial loops which are produced by displacement damage. In the Part I companion paper [1], it was shown that moving dislocations dissociated into Shockley partial dislocations during glide and such separation was increased with increasing radiation-induced defects such as Frank loops. The stacking violation in the region between the two separated partials produced twinned layers and caused a phase shift in the electron beam in transmission electron microscopy (TEM). The stacking violation was responsible for the observed twin bands and stacking fault ribbons. The twins formed by glide dislocations are generally several atomic layers thick, and are here called nanotwins. The remnant post-deformation glide dislocations constituted pile-up dislocations, observed extensively near grain boundaries. Defect-reduced channels were produced within the grains as a result of clearing of defects by the passage of Shockley partial dislocations, when hundreds to thousands of them passed through the glide planes successively.

An important implication of the separated Shockley partials is that an interaction between radiation-induced defects and a moving glide dislocation should occur by a two-step reaction, first with the leading partial and then with the trailing partial. Since **b** = [111]/3-type faulted Frank interstitial loops are sessile, the formation of **b** = [110]/2-type perfect glissile loops is a prerequisite for the removal of such defects. Thus, unfaulting of sessile loops is an important step in forming defect-reduced channels [1–6]. Previously it has been thought that an interaction occurs by a one-step reaction between a faulted Frank interstitial loop with **b** = [111]/3-type Burgers vector and a perfect dislocation with **b** = [110]/2-type Burgers vector or with an isolated Shockley partial with **b** = [112]/6-type Burgers vector [6–9]. Although glide dislocations are essentially all dissociated into Shockley partials in stainless steels and other low stacking fault energy f.c.c. materials, the presence of the trailing partial was largely overlooked in understanding deformation microstructure. Moreover, since glide dislocations extend all the way to grain boundaries or crystal surfaces, they affect not only the loops but also the area surrounding the loop, but such an effect was not considered. With this consideration, the genesis of deformation microstructures is reexamined in the following. In this paper, past work is reviewed only briefly to the extent required for discussion, since extensive reviews were already made in the cited references [2–9].

† Now with Honeywell Electronic Materials, 1349 Moffet Park Drive, Sunnyvale, CA 94089, USA.

‡ To whom all correspondence should be addressed. Tel.: +1-865-574-5058; fax: +1-865-574-0641.

E-mail address: farrellk@ornl.gov (K. Farrell)

1359-6454/01/$20.00 © 2001 Acta Materialia Inc. Published by Elsevier Science Ltd. All rights reserved.
PII: S1359-6454(01)00194-X

2. EXTENDED STACKING FAULTS

Although the nature of Shockley partial dislocations is well described in dislocation and mechanical property textbooks [10, 11], the role of partial dislocations on deformation mechanisms has not been clearly elucidated, particularly for irradiated materials. Moreover, although twin formation has been observed in almost all irradiated and deformed austenitic steels, its association with Shockley partial dislocations has not been often stated. Since the experimental evidence in Part I [1] revealed that all deformation microstructures were closely linked to Shockley partial dislocations, the relation between Shockley partial dislocations and deformation microstructures is reviewed here first.

As illustrated in Fig. 1, in an f.c.c. crystal, atoms are positioned on the saddle points of atoms on each successive (111) plane, B-atoms on the saddle points of A-atoms, C-atoms on the saddle points of B-atoms, etc. In the lowest energy packing, the C-atoms are placed not only on the saddle points of B-atoms but also on the saddle points of the second-order A-atoms below, as shown on the left in Fig. 1. In this stacking, the electron density overlap is least in the [111] direction. There are three non-equivalent atom positions viewed in projection as indicated by "A", "B" and "C" in the figure. On the "A" layer, there are two different saddle points, one is occupied by "B" atoms and the other is the unoccupied "C" position. At these empty saddle points, self-interstitial atoms can segregate to form an interstitial loop during irradiation. The interstitial atoms between the "A" and "B" layers become a mirror image with the C-atoms above the "B" layer. In this way, an interstitial loop forms initially in a faulted and twinned condition, although it can unfault to a perfect loop later.

On the (111) plane, atomic displacement in the $[10\bar{1}]$ direction or along the "hill" direction indicated by an arrow is difficult, so slip occurs by a zigzag path along the "valley" directions, such as $[11\bar{2}]/6$ plus $[2\bar{1}\bar{1}]/6$ displacements as shown in Fig. 1 and by equation (1). For simplicity, the unit lattice parameter "**a**" is omitted in all Burgers vector notations. Since the energy of a dislocation is proportional to $\mathbf{b}^2$, the energy relation of such a reaction is $2/4 > 6/36 + 6/36$.

$$\frac{1}{2}[10\bar{1}] \rightarrow \frac{1}{6}[11\bar{2}] + \frac{1}{6}[2\bar{1}\bar{1}] \qquad (1)$$

Therefore, a dissociation of a $[10\bar{1}]/2$ perfect dislocation into $[11\bar{2}]/6$ and $[2\bar{1}\bar{1}]/6$ Shockley partials lowers the energy and is energetically favorable.

When the atoms above the A-layer are displaced by a leading or zigging partial, all the atoms are still on the saddle points relative to the adjacent first-order layer atoms but not to those of the second-order layer atoms as shown by the middle stacking in Fig. 1. Now the previous B-atoms occupy C-atom positions and the previous C-atoms occupy A-atom positions, no longer located on the saddle points of the bottom A-atoms in second-order stacking, but instead locally forming a twin or mirror image across the middle C-layer (…**ACA**…). In this configuration, the A-atoms of the top and bottom layers are closer to each other and the electron density between them is more squeezed, raising the interfacial energy. This excess interfacial energy tends to displace faulted layers and becomes one of the driving forces in unfaulting a Frank loop, particularly when a loop becomes large.

The motion of a leading partial results in a shift in the displacement vector **R** by one-third in the [111] direction or by [111]/3, so the phase angle $\phi = 2\pi\mathbf{gR}$ can now have a fractional value. The definitions of diffracting vector (**g**) and displacement vector (**R**) can be found in Part I. An implication is that both twin and stacking fault fringes are an inherent consequence of a Shockley partial motion. In other words, both twins and stacking faults should always be seen if there is a region displaced by a leading partial. When the faulted region is displaced again by

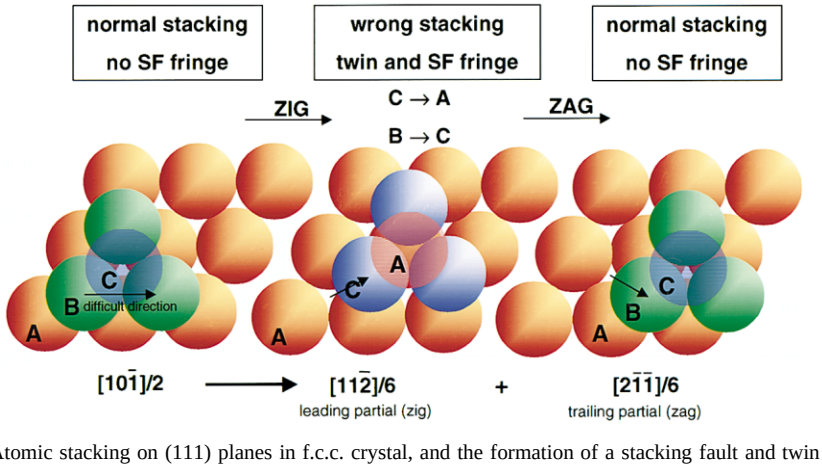

Fig. 1. Atomic stacking on (111) planes in f.c.c. crystal, and the formation of a stacking fault and twin by the displacement of a Shockley partial.

the trailing partial, normal lattice packing is restored leaving a slipped region behind as shown on the right of Fig. 1.

The partial dislocations repel one another to reduce the stress since they both have the same sign, while the driving force to minimize the surface area between the two partials or the surface excess free energy of the fault makes them attract one another. These two counteracting forces determine an equilibrium spacing of the two paired partials that depends on the specific stacking-fault energy. Stacking fault energy for austenitic stainless steel is relatively low (<10 mJ/m^2). Nevertheless, in unirradiated stainless steel, the separation of partial dislocations is generally so small (on the order of 10 to 20 **b**) that stacking fault regions are too narrow to be seen in most cases (see the top micrograph in Fig. 5 in Part I [1]). Fairly long stacking fault ribbons, however, have been observed occasionally because the leading partial often breaks away from the trailing partial when the latter is pinned by defects. In irradiated materials, the partials tended to separate with increasing irradiation dose as demonstrated in Fig. 5 in Part I [1]. The cause of separation of partial dislocations is discussed in Section 3.3.

In the irradiated stainless steel, the experimental evidence indicated that mechanical shear was accomplished largely by the successive motion of partial (or twinning) dislocations, each on a glide plane one or more interplanar spacings removed from its predecessor. The consequence of such displacement is examined schematically in detail here, by adopting the scheme described in Hirth and Lothe [10]. Figure 2(a) illustrates the atomic stacking sequences before and after displacement by a leading partial. When

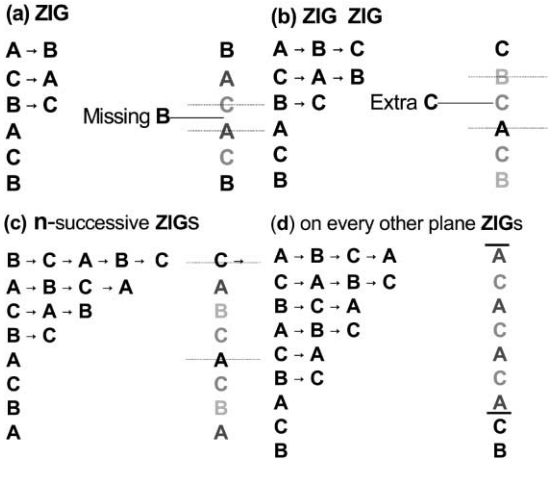

Fig. 2. (a) Intrinsic stacking fault produced by a partial dislocation motion. The fault has two one-layer nanotwins with two mirror planes. (b) Extrinsic stacking fault produced by two successive partial dislocation motions. The fault has two two-layer nanotwins with two mirror planes. (c) Coherent nanotwins are produced by *n*-successive partial dislocation motions. The fault has two *n*-layer nanotwins with two mirror planes. (d) Formation of h.c.p. packing by successive zig displacements of every other (111) plane. The dotted lines are mirror planes.

atoms are shifted by one zig motion, all atoms above the glide plane shift by one position as well, A to B, B to C, and C to A as illustrated in Fig. 2(a). The resulting stacking has two one-layer nanotwins and two mirror planes as indicated by the dotted lines. The new stacking can be seen to have one missing B-layer, so it is called an intrinsic stacking fault. Again it confirms that twins and stacking faults are both a consequence of the same partial dislocation motion.

Consecutive zig and zig motions on the same slip plane and in the same direction are energetically unfavorable because the second zig motion places the atoms on top of a "hill" and produces a high energy stacking such as …ABC**AA**BC… However, zig and zig motions on successive planes are possible as shown in Fig. 2(b). The resulting stacking has again two mirror planes but now the nanotwins are two layers thick (e.g. **BC**A**CB**). The stacking sequence has two missing layers or one extra C-layer, so is called an extrinsic stacking fault. The thickness of a twin layer increases with increasing number of zig displacements on successive planes as shown in Fig. 2(c). This produces a coherent nanotwin. Figure 3 shows examples of thin and thick nanotwins produced in 316LN austenitic stainless steel irradiated at 200°C to 1 and 20 at.% He with 360 keV He ions and strained to 10% by the disk bend method at room temperature. The rel-rod streaks in the diffraction pattern were more conspicuous for the thin layer twins as expected, whereas the streaks became more spotty as the twin layer thickened.

Strain-induced martensitic transformation has been observed for some austenitic stainless steels after deformation of both unirradiated and irradiated materials [12–15]. The formation of a martensitic phase was reported for J316 austenitic stainless steel neutron irradiated and tensile tested between 25 and 330°C [14]. During the examination of deformed disks under TEM in this work (Part I, [1]), it was also noticed that the electron beam tended to be deflected by a magnetic field from the TEM disk indicating that some martensitic phase might have formed during deformation. However, the martensitic phase appeared to be a very small fraction or too thin, since no identifiable diffraction patterns corresponding to a martensitic phase were observed by TEM. It was reported that an inhomogeneous shear of pre-existing or deformation-induced h.c.p. ϵ-phase can lead to the formation of a body-centered tetragonal martensitic structure known as α-phase [12]. As shown in Fig. 2(d), successive zig-displacements of every other plane can lead to the formation of an h.c.p. ϵ-phase region (…**ACACACA**…). However, the probability of forming a thick layer in this way is very small because of the random nature of slip during deformation.

As shown in Fig. 5 in Part I [1], a separation of partials was not conspicuous in unirradiated material. The trailing partial seemed to follow closely behind

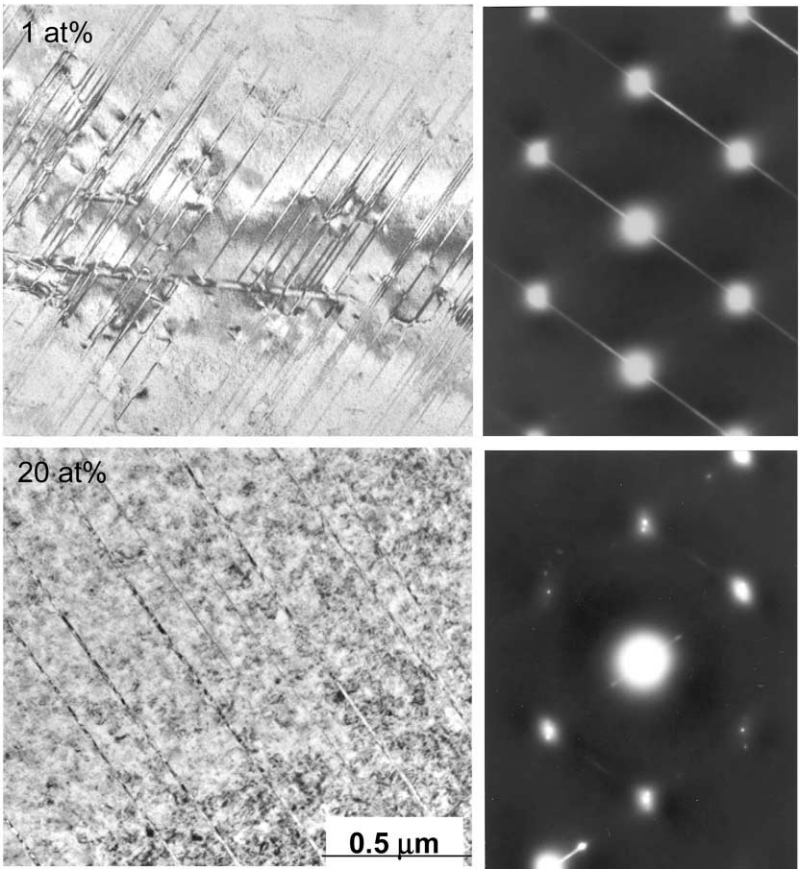

Fig. 3. Thin and thick nanotwins in 316LN austenitic stainless steel irradiated at 200°C to 1 and 20 at.% He with 360 keV He ions and strained to 10% by disk bend method at room temperature. The diffraction patterns and corresponding transmission electron micrographs are oriented in the same direction to show the relative orientation of the rel-rod streaks to the twin bands.

the leading partial during slip, in the absence of lattice defects. When the separation of Shockley partials was small, of course, both stacking faults and twins were not easily observable. With increasing ion dose, partials were separated due to dislocation pinning by a mechanism to be described later. This produced nanotwins, stacking faults, and/or h.c.p layers. Shear displacement was governed progressively by planar glide because it is difficult for widely separated partials or a faulted plane to cross-slip. Here, the term "planar glide" is used because the separated partial dislocations moved as a faulted plane on the slip plane. TEM diffraction patterns from twin bands showed streaks or twin spots depending upon the thickness of the twinned layers. Radiation-induced defects were cleared by interacting with glide dislocations, and also by a mechanism to be described in the next section. Hence, defect-reduced channel bands were produced on the glide planes.

The relation between dislocation motion and resulting microstructural features is summarized in Table 1. As listed in the bottom row of the table, deformation bands are a composite of all these features and thus have a complex internal structure in the bands. These are seen in TEM as pile-up dislocations, bands of stacking fault fringes, bands of twins, or bands of defect-reduced channel depending upon the imaging conditions. Nonetheless, they have the same origin. In unirradiated stainless steel, however, the separation of Shockley partial is not significant at low strain level, and thus dislocations glide readily with successive zigzag motion and cross-slip easily, producing random network dislocations.

3. LOOP UNFAULTING AND CHANNELING

In irradiated steels, profuse defect clusters, particularly Frank interstitial loops, are formed as a result of displacement damage. Cross-slip of both line and extended dislocations around these obstacles becomes difficult as their number and size increase and shear occurs predominantly by the movement of zigzagging partials along the energetically favorable $\langle 112 \rangle$ directions on close-packed {111} glide planes. However, application of suitably large stress can constrict the partial dislocations together against a barrier to form a whole dislocation and facilitate cross-slip. Such an incidence can lead to bifurcation of a channel band and becomes one of the mechanisms of widening a channel band. In general, the channel band

Table 1. Microstructures produced by Shockley partial dislocations

Partial motion	Faults	Twins (two mirror planes)	TEM	
			Image	Diffraction
ZIG↗ ZAG↘	no	no	dislocation line	normal
Successive ZIG↗ ZAG↘	no	no	dislocation line; channel band	normal
ZIG↗	intrinsic	one-layer nanotwins	dislocation line; SF fringes; twin band	streaks
ZIG↗ ZIG↗	extrinsic	two-layer nanotwins	dislocation line; SF fringes; twin band	streaks
ZIGs on *n*-successive planes	twin boundary	*n*-layer coherent nanotwins	dislocation line; SF fringes; twin band; channel band	twin spots
ZIGs on every other plane	h.c.p. stacking	nanotwins	dislocation line; SF fringes; twin band; h.c.p./martensite; channel band	streaks; h.c.p./bct spots
Combination of all the above	intrinsic; extrinsic; twin boundary; h.c.p.	single to multilayer nanotwins	dislocation line; SF fringes; twin band; h.c.p./martensite; channel band	streaks and twin spots

widths observed in stainless steel were narrower and the defect clearing was often less conspicuous than those observed in metals with higher stacking fault energy such as Cu and Al. The narrow and partially cleared channel bands in austenitic stainless steels are believed to be due to restricted cross-slip of widely separated Shockley partials and persistent Frank loops because of the low stacking fault energy.

In particular, during deformation, Frank loops are unfaulted and swept out by the stress field of glide dislocations from the same or adjacent slip planes, leaving cleared channels. The primary defect clearing mechanisms are considered to be first a removal of the stacking fault in the loop by interaction with deformation-induced moving dislocations, and subsequent elimination of the loop by prismatic glide from the slip band. However, detailed mechanisms have not been well understood, although there has been considerable interest in understanding how glide dislocations interact with Frank loops during deformation for austenitic stainless steels and other alloys irradiated in reactors [2–9]. The major effort has been focused largely on understanding the loop unfaulting and associated channeling mechanisms during deformation.

In general, two types of interactions are considered, Type I interaction for a moving dislocation and a loop on the same glide plane (e.g. the partials on a (111) plane interacting with the (111) loop, see Fig. 4), and Type II interaction for a moving dislocation and a loop on different glide planes (e.g. the partials on a $(\bar{1}\bar{1}1)$ basal plane interacting with a (111) loop, see Fig. 4) [8]. Type I includes an interaction of a Frank loop with a non-gliding dislocation such as an isolated Shockley partial nucleated inside the loop. However, the reaction with such a non-gliding isolated partial has not been clearly distinguished from the interaction with a gliding dislocation, although there exists a significant difference between the two mechanisms. In the following, therefore, the interaction mechanisms are considered in three separate categories.

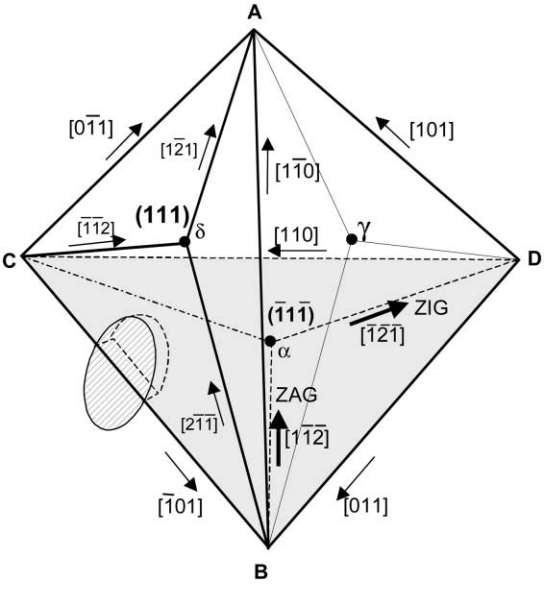

Fig. 4. Thompson tetrahedron to illustrate interactions between a moving dislocation and a **b** = [$\underline{1}\underline{1}\underline{1}$]/3 Frank interstitial loop: Type I interaction with the **b** = [$\bar{1}\underline{2}\underline{1}$]/6 Shockley partial on the (111) loop plane and a Type II interaction with the **b** = [121/6] leading and **b** = [112]/6 trailing partials on the shaded (111) basal plane. In all plane notations, the plane normal direction is away from the outside surface of the tetrahedron. To avoid congestion, fractional values of Burgers vectors are not included in the figure but are shown in the text.

3.1. Unfaulting by an isolated Shockley partial (Type I)

The faults of both intrinsic (vacancy) and extrinsic (interstitial) Frank loops can be removed, or a Frank loop can become a perfect loop by interacting with an isolated Shockley partial which is nucleated inside the Frank loop. Traditionally, this type of reaction is

assigned as Type I because both the loop and the interacting dislocation are on the same plane.

Before discussing the unfaulting mechanisms of a Frank loop, let us examine Fig. 2(a) and (b) by thinking of the missing "B" and the extra "C" layer as a vacancy and interstitial loop, respectively. Frank vacancy loops have one missing B-layer, and Frank interstitial loops have two missing layers (B and A) or one extra C-layer. As a consequence, in both cases, the C-layer is placed on top of the base A-layer or the C-positions are occupied such that any displacement in the "valley" direction on the A-plane will put the atoms on the empty B-position. Consequently, for the case of the Frank vacancy loop, a displacement of vacant sites places C to B, A to C, and B to A (note the reversing order of the displacements in unfaulting) and thus a normal ABC stacking is restored by one displacement. For the case of the Frank interstitial loop, however, two displacements are required to restore a normal stacking because of the additional stacking flaw above the loop.

Unfaulting of a Frank vacancy loop by a non-gliding partial or a coalescence mechanism has been considered previously [6–9]. Such a mechanism can be expressed by equation (2) by taking the $\mathbf{b} = [\bar{1}2\bar{1}]/6$ Shockley partial as a displacing vector for the vacant sites, for example:

$$\frac{1}{3}[\overline{111}] + \frac{1}{6}[\bar{1}2\bar{1}] \rightarrow \frac{1}{2}[\bar{1}0\bar{1}] \text{ or } \delta\mathrm{D} + \mathrm{A}\delta \rightarrow \mathrm{AD}. \tag{2}$$

The fault is removed and the vacancy loop is now a perfect and glissile loop with its Burgers vector parallel to the $[\bar{1}0\bar{1}]$ direction. Note that all vector conventions for a vacancy loop are opposite to those corresponding to an interstitial loop. One should be cautious that, in some literature, such a convention was often overlooked, resulting in some inconsistency in the analyses, for example by taking the same $[\bar{1}2\bar{1}]/6$ vector for both vacancy and interstitial loop. One should note that a vacancy loop unfaults when it displaces in the $[\bar{1}2\bar{1}]$ valley direction whereas an interstitial loop unfaults when it displaces in the $[1\bar{2}1]$ "hill" direction.

As can be seen in Fig. 5, for a $\mathbf{b} = [1\bar{1}1]/3$ Frank interstitial loop, a displacement in the $[\bar{1}2\bar{1}]/6$ direction encounters a "hill" or produces a higher energy stacking (**AA**C), and a displacement in any "valley" direction produces another stacking fault (**A**B**A**), so a displacement of a Frank interstitial loop in either "hill" or "valley" direction is energetically unfavorable. It has thus been suggested that when a Shockley partial encounters a "hill", it splits into two Shockley partials moving in separate directions, and unfaulting occurs by a synchronized shear of these two partials [16]. That is, when a force is applied on the loop atoms in a "hill" direction, the loop atoms are pushed aside in the "valley" direction and the atoms on top of the loop are jiggled back and forth sideways in response to the move—see the atom position along the vertical dotted line in Fig. 5. In this example, the $[1\bar{2}1]/6$ Shockley partial splits into $[2\overline{11}]/6$ and $[\overline{112}]/6$ partials when it encounters a "hill", and unfaulting is accomplished by a synchro-shear by $[\overline{112}]/6$ and $[2\overline{11}]/6$ partials. In this way, the loop atoms glide along the "valley" directions of both bottom and top atomic planes, synchronously. This process is written as follows:

$$\frac{1}{6}[1\bar{2}1] \rightarrow \frac{1}{6}[2\overline{11}] + \frac{1}{6}[\overline{112}] \text{ or } \delta\mathrm{A} \rightarrow \mathrm{B}\delta + \mathrm{C}\delta \tag{3}$$

$$\frac{1}{3}[111] + \frac{1}{6}[2\overline{11}] + \frac{1}{6}[\overline{112}] = \frac{1}{2}[101] \text{ or } \mathrm{D}\delta + \mathrm{B}\delta + \mathrm{C}\delta = \mathrm{DA}. \tag{4}$$

In effect, the Frank interstitial loop is shifted by one-half of the $[1\bar{2}1]/6$ distance as illustrated in Fig. 6(c, d). The loop atoms which were originally below the plane shown in the Fig. 6(c) are shifted up by $[\overline{112}]/6$ and appear on the plane shown in Fig. 6(d). The atoms on top of the loop in Fig. 6(c, d) shifted upward by $[\overline{112}]/6$ and downward by $[2\overline{11}]/6$, so they are still on the same plane and appear to be unchanged. This may cause some distortion around the loop which may be relieved to some degree by readjustment. A normal stacking is restored by repositioning the loop atoms from "C" to "B" and the atoms on top of the loop from "B" to "C", see Fig. 6(d). The loop atoms are now lined up with the matrix atoms parallel to the [101] direction. Therefore, the loop is now a perfect and glissile loop. Although all observable Frank loops formed in irradiated austenitic stainless steels are interstitial loops, unfaulting of a Frank vacancy loop is also shown in Fig. 6(a, b) for comparison. For the Frank vacancy loop, the direction of the shift is opposite to that of the Frank interstitial loop. That is, unfaulting of a vacancy loop occurs by simply shifting the "C" atoms on top of the loop to the "B" position, a "valley" direction.

The $\mathbf{b}^2$ relation for a Frank vacancy loop is equal before and after unfaulting as $3/9 + 6/36 = 2/4$ from equation (2). On the other hand, for a Frank interstitial loop, the $\mathbf{b}^2$ relation for the Shockley partial split raises the energy by a factor of two as $6/36 < 6/36 + 6/36$ from equation (3), although the overall Frank loop unfaulting process lowers the energy by one-sixth as $3/9 + 6/36 + 6/36 > 2/4$ from equation (4). Since large Frank vacancy loops have not been observed in irradiated austenitic stainless steels, the elevated interfacial energy by forming a loop itself appears to be sufficient enough to trigger unfaulting. In fact, Frank vacancy loops were found to unfault easily even at very small sizes and often collapse to vacancy tetrahedrons [17–19]. Such instability of vacancy loops is considered to be one of the reasons that

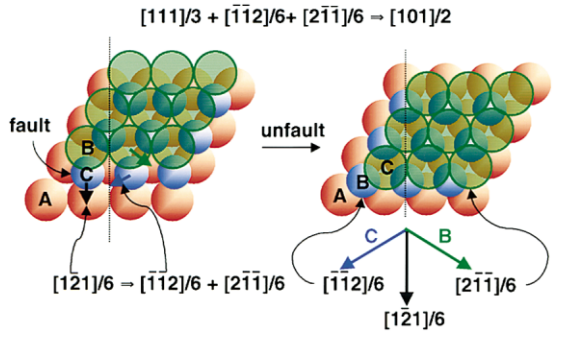

Fig. 5. The original $[1\bar{2}1]/6$ Shockley partial splits into $[\bar{1}\bar{1}2]/6$ and $[2\bar{1}\bar{1}]/6$ when it encounters a "hill". Unfaulting of an extrinsic Frank loop occurs by a synchro-shear of these two split Shockley partials.

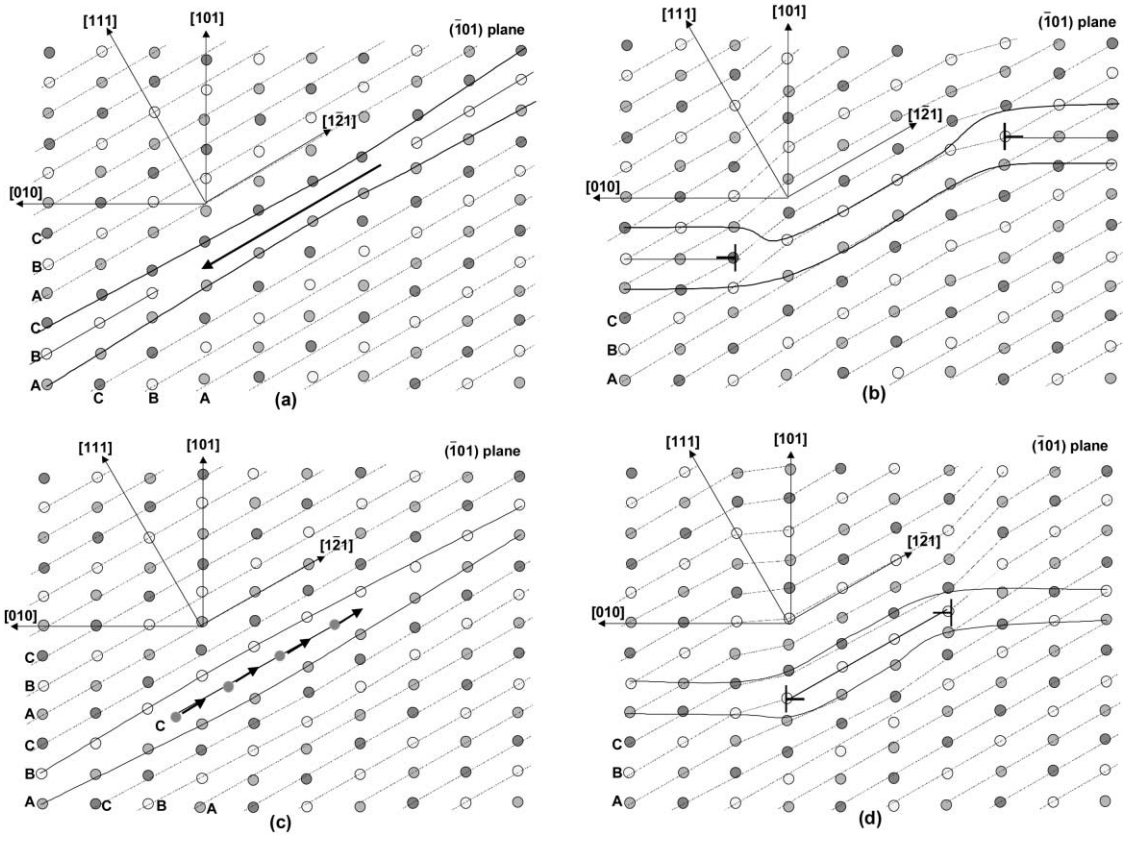

Fig. 6. Frank vacancy (a, b) and interstitial (c, d) loops before and after unfaulting. Atoms of (111) planes are seen edge-on in the (101) plane which is the paper plane. Note that the shift direction of the vacancy loop is opposite to that of the interstitial loop.

most remaining and observable loops after irradiation are of the interstitial type in austenitic stainless steel.

An isolated Shockley partial can be nucleated inside a Frank loop in various ways, which can then lead to unfaulting a loop [10]. Such events have been observed frequently in irradiated steels where glide dislocations are not directly involved. The nucleation of such a partial dislocation loop may occur by thermally activated processes, by condensation of vacancies on the loop during irradiation, or by the stress field of glide dislocations during deformation. As will be discussed later in detail, among these, the stress induced by pile-up dislocations plays a major role in unfaulting Frank loops during deformation. As mentioned earlier, a squeezed electron density between the faulted layers may produce a repulsive force and thus can cause a displacement of a faulted loop, particularly under applied stress. Since the path of such displacement should occur in an energetically favorable <112> "valley" direction, the unfaulting process is tantamount to a nucleation of a partial inside the loop.

Loop unfaulting triggered by a vacancy condensation process has been observed in 4.24 MeV proton-irradiated Fe–18Cr–14Ni austenitic stainless steel [6]. It was shown that a condensation of vacancies on the compression side of an interstitial loop nucleated vacancy loops with $\mathbf{b} = <112>/6$-type Burgers vector, and thus the fault inside the loop was eliminated without involving glide dislocations. A similar observation was made during *in situ* irradiation of Fe–16Cr–14Ni austenitic stainless steel with e-beam (1000 keV) or electron/He (300 keV) dual-beam in a high-voltage electron microscope [17, 18]. In the latter case, a complete unfaulting of interstitial loops was also observed without any involvement of glide dislocations or coalescence or growth of vacancy loops to eradicate the faulted loop. The vacancy loops collapsed to vacancy tetrahedrons when the interstitial loop was unfaulted. These results suggest that the annihilation of the fault was triggered by the vacancy loop with $\mathbf{b} = <112>/6$-type Shockley partial via a synchro-shear process. A driving force to reduce fault energy is also believed to play a role in such a process.

3.2. Unfaulting by coplanar glide Shockley partials (Type I)

In Section 3.1, unfaulting by an isolated Shockley partial was considered. However, when a Frank loop is interacting with a glide dislocation on the same glide plane, most likely during deformation, the situation becomes more complicated. Since a glide dislocation is extended throughout the grain and cannot be terminated inside the grain unless it is a closed loop, it displaces not only the loop atoms but also the atoms surrounding the loop as illustrated in Fig. 7. As the leading partial encounters loop atoms, it displaces them, and accordingly the atoms above the loop are also repositioned to a lower energy configuration by the synchro-shear mechanism stated above. A difference is that, at the same time, the atoms surrounding the loop are also displaced by the $[1\bar{2}1]/6$ Shockley partial. As a consequence, a normal stacking is restored in the loop region by the equation (4) reaction, while the area surrounding the loop becomes faulted by the twinning leading partial.

When the trailing partial passes over this area, the loop becomes faulted again by a synchro-shear process, while normal stacking is restored in the matrix.

$$\frac{1}{2}[101] + \frac{1}{6}[2\bar{1}\bar{1}] = \frac{1}{6}[5\bar{1}2] \text{ or } \mathrm{DA} + \mathrm{B}\delta = \mathrm{D}\delta + \mathrm{BA}. \quad (5)$$

The split of Shockley partial for synchro-shear is not elaborated in the above equation. The resulting faulted loop now has a high index Burgers vector $\mathbf{b} = [5\bar{1}2]/6$, but it is nothing but the same faulted $\mathbf{b} = [111]/3$ loop which is shifted by $[1\bar{1}0]/2$ as can be seen by equation (6) below. This is already indicated in Thompson notation of equation (5) above.

$$\frac{1}{6}[5\bar{1}2] = \frac{1}{3}[111] + \frac{1}{2}[1\bar{1}0] \quad (6)$$

An implication is that a Frank loop would not unfault by a glide dislocation by Type I reaction unless the prismatic loop formed by the leading partial glides away from the slip plane before encountering the trailing partial. Although a perfect loop in a perfect lattice is known to be removed easily by a prismatic glide, a perfect loop in a faulted layer may not. In particular, when the separation of Shockley partials is smaller than the size of a loop, only the area between the leading and trailing partials is unfaulted as they pass through and the loop would remain sessile. For this reason, Type I interaction with glide dislocations is considered to be inefficient in unfaulting a loop. However, since the formation of $\mathbf{b} = [5\bar{1}2]/6$-type high index loops would require an additional energy in shifting the $\mathbf{b} = [111]/3$-type loop by $[1\bar{1}0]/2$, such interactions could be a strain hardening factor.

Moreover, the incidence of Type I interaction with glide dislocations would be very low because the probability for a moving dislocation encountering a loop on the same glide plane is very low compared to that for Type II interaction in which the entire loop area is subjected to many moving dislocations on slip planes. Furthermore, the number of dislocations available for Type I interaction is one third of that for Type II, because a Type I loop interacts with dislo-

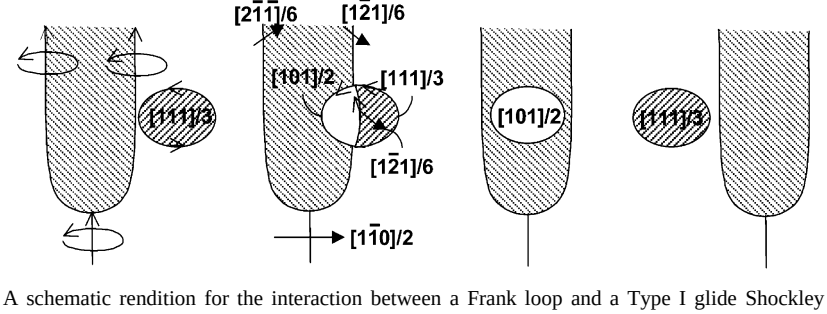

Fig. 7. A schematic rendition for the interaction between a Frank loop and a Type I glide Shockley partial. One can confirm that the summation of the three (not four) Burgers vectors at the nodal points leads to zero, according to the Frank rule.

cations on the same glide plane whereas a Type II loop interacts with dislocations from three non-loop-containing glide planes.

At this time, we have not identified an example to show an unfaulted loop inside a stacking faulted layer. This is mainly because loop sizes observed in this work are mostly too small to resolve an unfaulted condition and secondly the probability to produce such a loop is low for the reasons mentioned above. It would be interesting to design an experiment to produce large loops by irradiating at elevated temperature and study loop microstructure after deformation.

3.3. Unfaulting by non-coplanar glide Shockley partials (Type II)

Under stressed conditions, when the trailing partial remains pinned, the leading partial can break away, widening the gap between the two pairing partials and forming a stacking faulted region between them. Among several mechanisms, Cottrell locking (i.e. the locking by the atmosphere of solute atoms that segregate near the core of a dislocation) and Suzuki locking (i.e. the locking of extended dislocations by solute atoms that segregate to a stacking fault) are considered to be dominant factors in causing the separation of partial dislocations [10]. However, since Cottrell locking may occur equally for both leading and trailing partials, a preferential pinning of the trailing partial is not expected and thus the systematic separation of Shockley partials cannot be explained. Suzuki locking can lead to a separation of Shockley partials by a drag-type behavior resulting from segregation along a gliding dislocation. Again, however, the dose-dependent nature of the separation (Fig. 5 in Part I, [1]) cannot be explained because the average alloy composition would not change by radiation, even though there might be some redistribution of solutes. Moreover, diffusion of solute atoms may not play a significant role during post-irradiation deformation, particularly at low temperatures. Discussed below is a new mechanism consistent with the experimental findings.

As pointed out already, an interaction between a loop and a glide dislocation occurs in two steps, first with the leading partial and then with the trailing partial. In this example, an interaction occurs between a $\mathbf{b} = [111]/3$ loop and glide partials, $[\bar{1}2\bar{1}]/6$ and $[1\bar{1}2]/6$, on the $(11\bar{1})$ basal plane, see Fig. 4. An interaction with the leading partial $[\bar{1}2\bar{1}]/6$ results in the formation of a partial dislocation with $\mathbf{b} = [101]/6$ Burgers vector on the jogged section of a loop as shown in Fig. 8. The associated dislocation reaction is

$$\frac{1}{3}[111] + \frac{1}{6}[\bar{1}2\bar{1}] = \frac{1}{6}[102] \text{ or } \mathrm{D}\delta + \alpha\mathrm{D} = \alpha\delta. \tag{7}$$

The $\mathbf{b} = [101]/6$ partial is neither on the (111) loop plane (dot product $[111]\cdot[101] \neq 0$), nor is it in the direction of the $[\bar{1}01]$ line vector (**CB** direction), but is placed on a (100) plane which is not a glide plane. The plane of the short jogged loop is the same as the glide plane as can be confirmed by the cross-product, $[121]\times[\bar{1}01] = 2[1\bar{1}\bar{1}]$ or $[\bar{1}2\bar{1}]\times[\bar{1}01] = 2[\bar{1}\bar{1}\bar{1}]$ depending upon the loop normal direction taken. The Burgers vector of the jogged section is always parallel to or the same as the Burgers vector of the moving dislocation. Hence, the Burgers vector of the jogged section is $\mathbf{b} = [\bar{1}2\bar{1}]/6$ which is the direction of the moving partial. It should be mentioned that any zig-displacement without an accompanying zag-displacement produces a stacking faulted region as demonstrated in Fig. 2, and thus the short jogged $\mathbf{b} = [1\bar{1}\bar{1}]/3$ loop is faulted. The twinning leading partial also leaves a faulted region behind along its passage in the matrix around the short jogged section. If glide dislocations pass through the same glide plane again and again, the jogged section elongates continuously. Such a case was observed during *in situ* deformation of proton-irradiated Fe–18Cr–14Ni austenitic stainless steel [5].

The original $\mathbf{b} = [111]/3$ loop and the newly formed jogged $\mathbf{b} = [1\bar{1}\bar{1}]/3$ loop are both sessile because the Burgers vectors are not on glide planes. The dislocation formed at the intersection of two such planes is called a stair-rod partial for its geometric shape ([9], p. 303). In Thompson notation, the stair-rod partial in this example can be identified by two Greek letters as "$\alpha\delta$". The stair-rod dislocation resists both climb and glide forces and thus is often called a supersessile dislocation. As a consequence, the trailing partial experiences a greater resistance when it encounters the strain field of the stair-rod partial than the leading partial interacting with an unjogged loop.

Since the energy relation ($\mathbf{b}^2$ value) for the reactants and product dislocations of equation (7) gives $3/9 + 6/36 \gg 2/36$, the reaction is energetically favorable. Although the opposite sense of the stair-rod dipole partials makes them attract one another, in view of the large reduction in the product $\mathbf{b}^2$, it is probable that some non-vanishing length of stair-rod remains after the leading partial passes through the loop. As pointed out already, both the Frank partial and the stair-rod partial are sessile. Therefore, a separation of Shockley partials is likely to occur when the movement of the trailing partial is impeded by the jogs and stair-rod partials. For this reason, an increasing separation of Shockley partials occurs with increasing number density and size of Frank loops. Since the presence of jogs themselves makes the dislocations containing them less mobile, a similar result may occur when jogs are produced by a leading partial on the dislocations on a glide plane. Moreover, the direction of the leading and trailing partials are off by 60°, and thus the jogs formed by a leading partial are not in a favorable direction to the trailing partial and are likely to become a stronger barrier. These facts may account for the formation of profuse stacking-faults in heavily cold-worked alloys as

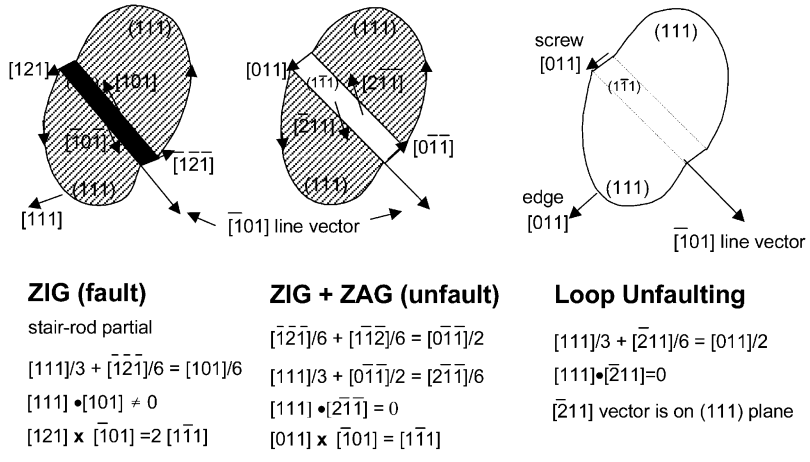

Fig. 8. Type II interaction between a Frank loop and a glide Shockley partial dislocation. The reaction occurs in two steps. The leading partial produces a faulted small loop with stair-rod partials, and the trailing partial unfaults the jogged loop and produces Shockley partials inside the loop. The interaction of these Shockley partials with each of the sheared half loops can unfault the loop.

shown in Fig. 9 in Part I [1]. This process is thus considered to contribute to the extensive fault formation in the highly strained condition for both irradiated and unirradiated steels.

As mentioned already, in Type II interaction, when a moving dislocation encounters a loop, the partials are separated due to the jog-pinning and stair-rod locking. However, if stress concentration exceeds a certain critical value, the trailing partial can also break away. It should be noted that a zig motion produces a fault and a zag motion removes the fault. Thus the zigzag pass through a loop produces a small unfaulted loop with jogs on a slip plane as indicated by unshading in the rectangular region of the middle loop in Fig. 8. The reaction between the $\mathbf{b} = [111]/3$ loop and the zigzag partials ($[\bar{1}2\bar{1}]/6 + [112]/6 = [0\bar{1}\bar{1}]/2$) can be written, without detailing the two split partials, simply as

$$\frac{1}{3}[111] + \frac{1}{2}[0\bar{1}\bar{1}] = \frac{1}{6}[2\bar{1}\bar{1}] \text{ or } D\delta + BD = B\delta. \tag{8}$$

The Burgers vectors of the newly formed partial in the jogged loop are $\mathbf{b} = [2\bar{1}\bar{1}]/6$ and $[\bar{2}11]/6$ which are now on the (111) loop plane (i.e. $[111]\cdot[2\bar{1}\bar{1}] = 0$) and so they can glide on the loop plane. The original Frank loop can thus be unfaulted by the following dislocation interaction:

$$\frac{1}{3}[111] + \frac{1}{6}[\bar{2}11] = \frac{1}{2}[011] \text{ or } D\delta + \delta B = DB. \tag{9}$$

The $\mathbf{b} = [011]/2$ dislocation at the jogged section is parallel to the slip direction so it is a screw dislocation and the Burgers vector of the unfaulted loop is also [011]/2, and thus the loop can be removed by prismatic glide. The values of $\mathbf{b}^2$ for the reactants and the product for equation (9) are equal (i.e. 3/9 + 6/36 = 2/4) and thus the reaction has no advantage in terms of $\mathbf{b}^2$. However, the reaction would reduce the stacking fault energy and thus the reaction may occur if the dipoles move away in opposite directions under stressed conditions. Nonetheless, jogged loops are less mobile than unjogged ones. This may have been the reason for the low efficiency in removing faulted loops during *in situ* deformation of proton-irradiated Fe–18Cr–14Ni austenitic stainless steel [6]. Since both Type I and Type II interactions with glide dislocations are found to be inefficient in removing defects, unfaulting by isolated Shockley partials (i.e. partials nucleated inside the loop by stress field or vacancy condensation) is considered to be a dominant mechanism for defect-reduced channel formation.

4. CONCLUSIONS

The origin of deformation microstructures was clarified by analyzing the nature of Shockley partial dislocations and their interaction with radiation-induced Frank loops. Deformation produces glide dislocations which are essentially pairs of Shockley partial dislocations, and thus an interaction between a glide dislocation and radiation-induced defects occurs by a two-step reaction, first with a leading partial and then with the trailing partial. This two-step interaction mechanism is elucidated for the first time in this work.

Analyses revealed that a Type II interaction of a Frank loop with a leading Shockley partial produces jogs and stair-rod partials on the loop, which in turn impede the motion of the trailing partial. With increasing radiation-induced defects, therefore, partials are separated further by jog-pinning and stair-rod locking. Consequently, cross-slip is suppressed and planar glide enhanced. Nanotwins and stacking fault

ribbons are the result of the stacking violation between these two separated partials. During deformation, Frank loops unfault by the stress of pile-up dislocations and are removed from the slip bands. Such processes produce defect-reduced channel bands. In this way, pile-up dislocations, stacking fault ribbons, twin bands, and defect-reduced channels are inherently linked together.

Three modes of unfaulting were considered for Frank loops: the nucleation of a Shockley partial inside the loop with no direct involvement with glide dislocations; interaction between a Frank loop and a glide dislocation on the same plane; and interaction between a Frank loop and a glide dislocation on a different glide plane. Among the three mechanisms, unfaulting by glide dislocations was found to be inefficient, particularly for the case of interaction with coplanar glide dislocations. Unfaulting of a Frank loop is thus believed to occur mostly by the stress-induced nucleation of a Shockley partial inside the loop during deformation.

Literature data and our ongoing work indicate that the above-mentioned deformation mechanisms operate for AISI 316LN-type austenitic stainless steels from liquid nitrogen temperature up to a temperature ($\lesssim$500°C) where dislocation motion is controlled by thermally activated processes. Therefore, the observed deformation characteristics are attributable largely to the nature of the f.c.c. crystal structure and low stacking fault energy of austenitic stainless steel. However, different mechanisms may operate at extremely low temperatures or very fast strain rate conditions, or for f.c.c. materials with higher stacking fault energy, or for materials with different crystal structure. Other materials will be studied in the future using detailed dislocation analyses similar to the present work.

Acknowledgements—Research sponsored by the Division of Materials Sciences and Engineering, Office of Basic Energy Sciences, US Department of Energy, under contract no. DE-AC05-00OR22725 with UT-Battelle, LLC. The authors thank Drs E. A. Kenik and S. J. Zinkle for reviewing the manuscript.

REFERENCES

1. Lee, E. H., Byun, T. S., Hunn, J. D., Yoo, M. H., Farrell, K. and Mansur, L. K., *Acta mater.*, 2001, **49**(16), 3269–3276.
2. Sharp, J. V., *Phil. Mag.*, 1967, **16**, 77.
3. Sharp, J. V., *Acta metall.*, 1974, **22**, 449.
4. Bruemer, S. M., Cole, J. I., Carter, R. D. and Was, G. S., *Mater. Res. Soc. Symp. Proc.*, 1997, **439**, 437.
5. Cole, J. I. and Bruemmer, S. M., *J. Nucl. Mater.*, 1995, **225**, 53.
6. Suzuki, M., Sato, A. and Mori, T., *Phil. Mag.*, 1992, **65**, 1039.
7. Gelles, D. S., in *Dislocation Modeling of Physical Systems*, ed. M. F. Ashby, R. Bullough, C. S. Hartley and J. P. Hirth. Pergamon Press, New York, 1980, p. 158.
8. Song, S. G., Cole, J. I. and Bruemmer, S. M., *Acta mater.*, 1997, **45**, 501.
9. Yoo, M. H. and Hishinuma, A., in *Advances in Twinning*, ed. S. Ankem and C. S. Pande. The Minerals, Metals and Materials Society, College Park, Maryland, 1999, p. 226.
10. Hirth, J. P. and Lothe, J., *Theory of Dislocations*. McGraw-Hill Book Company, New York, 1968, pp. 288, 307, and 751.
11. Meyers, M. A. and Chawla, K. K., *Mechanical Behavior of Materials*. Prentice Hall, New Jersey, 1999.
12. Venables, J. A., *Phil. Mag.*, 1962, **7**, 35.
13. Fahr, D., *Metall. Trans.*, 1971, **2**, 1883.
14. Choi, H. C., Ha, T. K., Shin, H. C. and Chang, Y. W., *Scripta mater.*, 1999, **40**, 1171.
15. Hashimoto, N., Zinkle, S. J., Rowcliffe, A. F., Robertson, J. P. and Jitsukawa, S., *J. Nucl. Mater.*, 2000, **283–287**, 528.
16. Weertman, J. and Weertman, J. R., *Elementary Dislocation Theory*. The Macmillan Company, London, UK, 1964, p. 103.
17. Takahashi, H., Hidaka, Y. and Ohnuki, S., *Micron*, 1996, **27**, 239.
18. Hidaka, Y., Ohnuki, S., Takahashi, H. and Watanabe, S., *J. Nucl. Mater.*, 1994, **212-215**, 330.
19. Horiki, M. and Kirtani, M., *J. Nucl. Mater.*, 1994, **212-215**, 246.